Resource

Molecular Cell

Circular RNAs in the Mammalian Brain Are Highly Abundant, Conserved, and Dynamically Expressed

Graphical Abstract

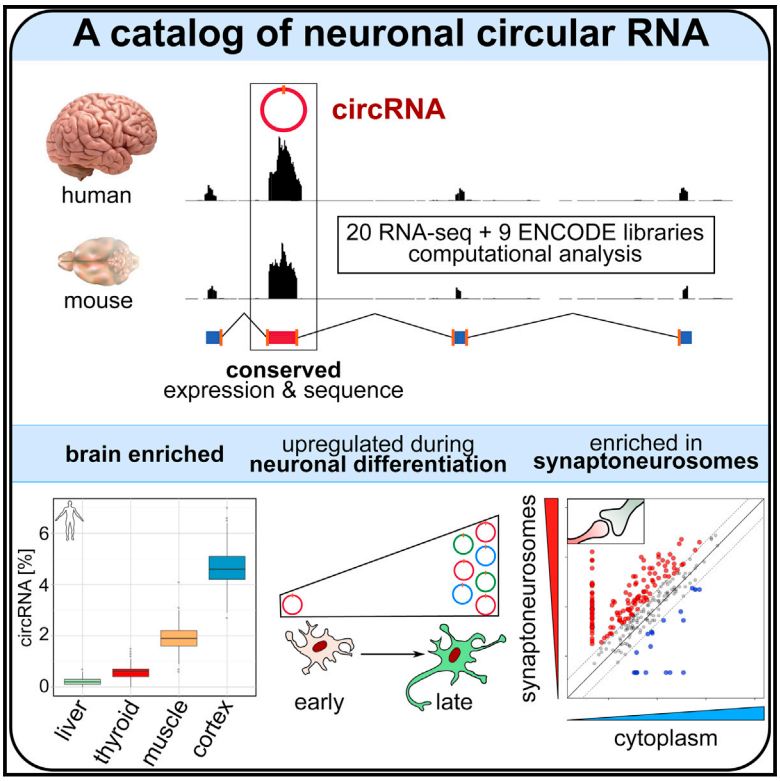

Authors

Agnieszka Rybak-Wolf, Christin Stottmeister, ..., Sebastian Kadener, Nikolaus Rajewsky

Correspondence

rajewsky@mdc-berlin.de

In Brief

Rybak-Wolf et al. combined computation and experiment to compile a catalog of circRNA expression in the brain. circRNAs are highly enriched in the mammalian brain, with specific and dynamic expression during neuronal differentiation, often independent of linear transcripts. Brain-expressed circRNAs are often conserved in expression and display elevated sequence conservation.

Highlights

- circRNAs are highly abundant in the mammalian brain and enriched in synaptoneurosomes
- circRNAs are upregulated during neuronal differentiation
- Many circRNAs show dynamic expression, independent of linear transcript dynamics
- Neuronal circRNAs are significantly conserved in expression and sequence

Accession Numbers

GSE65926

Rybak-Wolf et al., 2015, Molecular Cell *58*, 870–885
June 4, 2015
http://dx.doi.org/10.1016/j.molcel.2015.03.027

CellPress

Molecular Cell
Resource

Circular RNAs in the Mammalian Brain Are Highly Abundant, Conserved, and Dynamically Expressed

Agnieszka Rybak-Wolf,[1,6] Christin Stottmeister,[1,6] Petar Glažar,[1,6] Marvin Jens,[1] Natalia Pino,[4] Sebastian Giusti,[4] Mor Hanan,[2] Mikaela Behm,[3] Osnat Bartok,[2] Reut Ashwal-Fluss,[2] Margareta Herzog,[1] Luisa Schreyer,[1] Panagiotis Papavasileiou,[1] Andranik Ivanov,[1] Marie Öhman,[3] Damian Refojo,[4,5] Sebastian Kadener,[2] and Nikolaus Rajewsky[1,*]

[1]Systems Biology of Gene Regulatory Elements, Max-Delbrück Center for Molecular Medicine, Robert-Rössle-Strasse 10, 13125 Berlin, Germany

[2]The Alexander Silberman Institute of Life Sciences, The Hebrew University of Jerusalem, Edmond J. Safra Campus, Jerusalem 91904, Israel

[3]Department of Molecular Biosciences, The Wenner-Gren Institute, Stockholm University, 106 91 Stockholm, Sweden

[4]Molecular Neurobiology, Max Planck Institute of Psychiatry, 80804 Munich, Germany

[5]Instituto de Investigación en Biomedicina de Buenos Aires (IBioBA), CONICET – Partner Institute of the Max Planck Society, C1425FQD Buenos Aires, Argentina

[6]Co-first author

*Correspondence: rajewsky@mdc-berlin.de

http://dx.doi.org/10.1016/j.molcel.2015.03.027

SUMMARY

Circular RNAs (circRNAs) are an endogenous class of animal RNAs. Despite their abundance, their function and expression in the nervous system are unknown. Therefore, we sequenced RNA from different brain regions, primary neurons, isolated synapses, as well as during neuronal differentiation. Using these and other available data, we discovered and analyzed thousands of neuronal human and mouse circRNAs. circRNAs were extraordinarily enriched in the mammalian brain, well conserved in sequence, often expressed as circRNAs in both human and mouse, and sometimes even detected in *Drosophila* brains. circRNAs were overall upregulated during neuronal differentiation, highly enriched in synapses, and often differentially expressed compared to their mRNA isoforms. circRNA expression correlated negatively with expression of the RNA-editing enzyme ADAR1. Knockdown of ADAR1 induced elevated circRNA expression. Together, we provide a circRNA brain expression atlas and evidence for important circRNA functions and values as biomarkers.

INTRODUCTION

Circular RNAs (circRNAs) have recently emerged as a large class of animal RNAs (Hansen et al., 2013; Jeck and Sharpless, 2014; Jeck et al., 2013; Lasda and Parker, 2014; Memczak et al., 2013; Salzman et al., 2012, 2013) with complex tissue- and stage-specific expression patterns. circRNAs are much more stable than linear RNAs and therefore might be involved in different functions. The human circRNA CDR1as has recently been identified as a negative regulator ("sponge") of the microRNA miR-7 (Hansen et al., 2013; Memczak et al., 2013), demonstrating the regulatory potential of circRNAs.

circRNAs are thought to be predominantly produced by back-splicing reactions that covalently link the 3′ end of an exon to the 5′ end of an upstream exon (Ashwal-Fluss et al., 2014; Zhang et al., 2014; Starke et al., 2015). Recent studies have provided evidence that in mammals, reverse complementary sequences that reside in the introns flanking circularized exons promote circRNA biogenesis (Ashwal-Fluss et al., 2014; Liang and Wilusz, 2014; Zhang et al., 2014; Ivanov et al., 2015; Starke et al., 2015), as originally found for the SRY circRNA (Capel et al., 1993; Dubin et al., 1995). After transcription, such intronic sequences can base pair, bringing together 5′ and 3′ ends of the circularized exons. A prediction of this model is that the respective reverse complementary sequences should be targeted by the ADAR editing enzymes (Ivanov et al., 2015). Indeed, adenosine-to-inosine (A-to-I) editing events are enriched in these sequences, and knockdown of ADAR1 in a human cell line induced modest upregulation of circRNAs (Ivanov et al., 2015).

It has also been shown that Muscleblind, a conserved regulator of alternative splicing, promotes circularization of one of its own exons by binding to flanking intronic sequences, leading to an order of magnitude higher expression of the *musclebind* circRNA compared to the linear mRNA in fly heads (Ashwal-Fluss et al., 2014). CDR1as, perhaps the best-characterized mammalian circRNA, is also highly abundant in neurons (Hansen et al., 2011; Memczak et al., 2013). Moreover, it has been noticed that neural genes often express circRNAs (Ashwal-Fluss et al., 2014), and that *Drosophila* neural tissues are highly enriched in circRNAs (Westholm et al., 2014) compared to other tissues. In flies, circRNAs also accumulate during aging of the brain, indicating interesting functions of circRNAs in this process (Westholm et al., 2014). Consistently, these circRNAs are highly significantly conserved across *Drosophila* species (Westholm et al., 2014). These observations lead us to systematically investigate the expression of circRNAs in mammalian neural cells.

In mammals, A-to-I editing is known to increase during brain development (Shtrichman et al., 2012; Wahlstedt et al., 2009).

However, ADAR1 editing of inverted Alu repeats has been shown to be highly regulated during differentiation of stem cells toward neural fate (Osenberg et al., 2010). We were therefore interested in studying a possible regulatory role of ADAR1 in the biogenesis of neural circRNAs.

To systematically identify and analyze circRNAs in neural tissues, we followed our previous approach, i.e., sequencing ribosomal-depleted RNA, subsequent computational analyses, which uncover head-to-tail junctions (Glažar et al., 2014; Memczak et al., 2013), and experimental validation. We used established cell culture systems for neuronal differentiation, mouse P19 embryonic carcinoma (EC) and human neuroblastoma SH-SY5Y cells (McBurney, 1993; Monzo et al., 2012; Ross et al., 1983), in which multipotent cells, after retinoic acid treatment, acquire neuronal identity. We complemented this system with embryonic primary mouse neuronal cultures, an established method to assess neuronal maturation. We also extracted total RNA from murine synaptoneurosome fractions (Gray and Whittaker, 1960; Huttner et al., 1983) and different parts of the postnatal mouse brain. For human, we took advantage of recently published sequencing data from the ENCODE Project Consortium (Bernstein et al., 2012) and used SH-SY5Y-derived neuronal cells (Ross et al., 1983). To study the role of ADAR1 in neuronal differentiation, we knocked down ADAR1 in the P19 and SH-SY5Y cells.

Our data revealed that circRNAs are highly abundant in mammalian brain compared to other analyzed tissues. The majority of detected mouse circRNAs were also expressed as circRNAs in human brain, and some of them even detected in *Drosophila* brains. Strikingly, the nucleotide sequence of circRNAs was significantly better conserved than the sequences of the flanking exons. circRNAs were overall upregulated during neuronal differentiation and development, highly enriched in synapses, and in some cases showed differential expression compared to their linear isoforms. Interestingly, their elevated expression correlated negatively with ADAR1 expression, both in flies and mammals. Moreover, knockdown of ADAR1 in cell culture upregulates specific circRNAs, suggesting that ADAR1 can repress the biogenesis of neuronal circRNAs. Taken together, this is a first systematic analysis of circRNA expression profiles in mammalian brains, and an important step toward further elucidation of circRNA functions in the CNS.

RESULTS

circRNAs Are Highly Abundant in Mouse and Human CNS

Our overall strategy is summarized in Figure 1A. Total RNA was extracted, depleted from rRNA, and sequenced using standard protocols (see Experimental Procedures and Supplemental Experimental Procedures). Head-to-tail junctions were detected as previously described (Glažar et al., 2014; Memczak et al., 2013). Putative splice sites were defined based on the genome reference only, without relying on genome annotation, and were filtered on a number of quality criteria (see Supplemental Computational Procedures).

The number of reads spanning the head-to-tail junction was used to quantify circular expression. To normalize for sequencing depth of the respective libraries and the efficiency of rRNA depletion, we also estimated the expression of a circRNA relative to the expression of its linear isoforms. As a conservative (upper bound) estimate for the total expression of all linear transcripts that contain the same exons as a circRNA, we selected the maximum of linearly spliced read counts at the 5′ and 3′ splice sites of the circRNA (Quantification module, Figure 1A; Supplemental Computational Procedures).

Figure 1B summarizes all cell culture time courses, synaptoneurosomes, and brain samples that we collected for this study, including available mouse and human brain data from the ENCODE Project Consortium (Bernstein et al., 2012).

In total, we detected 15,849 distinct circRNA candidates in mouse and 65,731 in human brain samples (Table S1), with at least two uniquely aligning, distinct read sequences supporting the head-to-tail junction. The higher number of human circRNA candidates may partially be explained by the higher sequencing depth. A total of 90% of mouse and 73% of human circRNAs were not annotated in circBase (Glažar et al., 2014) to date. A detailed summary for each sample is provided in Table S2. While the majority of head-to-tail junctions were supported by few reads (two to ten), we also detected 565 mouse and 5,962 human circRNAs supported by more than 100 junction-spanning reads (Figure 1C). Brain-expressed circRNAs were usually derived from annotated exons, with a clear preference for coding sequence (CDS) and 5′ UTR exons (Figure 1C, inset). Their splice sites typically enclose three exons. While the median number of circRNAs per gene in human brain samples is three, 2,338 genes give rise to ten or more circular isoforms. The number of such genes was lower in mouse (163), with a median number of two circRNA isoforms. Interestingly, 4.2% (10.8%) of all human (mouse) circRNAs aligned antisense to known transcripts.

We found hundreds of circRNAs that are expressed several times higher than their canonical/linear isoform. Most of these arise from the annotated splice sites of well-expressed transcripts, and are often strikingly easy to observe from the RNA-seq coverage (Figure S1H).

To independently test these results, we selected ten mouse circRNA candidates with different expression levels. All proved resistant to the 3′-to-5′ exonuclease RNase R, validating circularity (Figures S1A and S1B). For five candidates we further directly compared linear and circRNA resistance to RNase R by northern blots using probes recognizing both isoforms (Figure S1C), avoiding any amplification (reverse transcription and PCR). All candidates showed higher RNase R resistance than the linear isoforms. Next, we assayed the head-to-tail splicing by RT-PCR with divergent primers and by Sanger sequencing (Figures S1D and S1E). We also used short (~100 nt) RNA probes spanning the head-to-tail junction for circRNA-specific (see below; Figure S2A) northern blotting and validated brain expression of 7/7 mouse candidates (Figure 1D).

As many brain circRNAs appeared highly expressed, we compared human frontal cortex, thyroid gland, liver, and muscle and found an overall enrichment for circRNA expression in the nervous system (see Supplemental Computational Procedures; Figure 1E). The same was observed in mouse (data not shown).

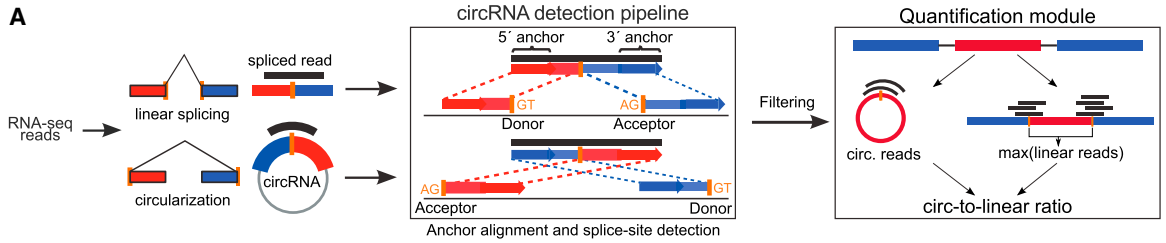

B

organism	sample	# circRNAs	# circ > lin
mouse	brain developmental stages [TS]	*validation only*	
	cerebellum [TS]	2,407	238 (9.9 %)
	pre-frontal cortex [TS]	1,677	166 (9.9 %)
	hippocampus [TS]	1,212	164 (13.5 %)
	olfactory bulb [TS]	1,771	189 (10.3 %)
	P19 differentiation [TS]	2,735	508 (18.6 %)
	post-natal forebrain [E]	6,614	1,182 (17.9 %)
	post-natal hindbrain [E]	3,382	1,055 (31.2 %)
	post-natal midbrain [E]	3,758	1,033 (27.5 %)
	primary cortical neurons [TS]	5,265	646 (12.3 %)
	synaptoneurosomes [TS]	1,773	317 (17.9 %)
human	cerebellum [E]	21,071	2,289 (10.9 %)
	diencephalon [E]	24,632	2,430 (9.9 %)
	frontal cortex [E]	38,983	4,089 (10.5 %)
	occipital lobe [E]	31,085	3,410 (11.0 %)
	parietal lobe [E]	23,303	2,159 (9.3 %)
	temporal lobe [E]	21,835	2,718 (12.4 %)
	SH-SY5Y differentiation [TS]	4,264	639 (15.0 %)

[TS]- this study [E]- ENCODE data

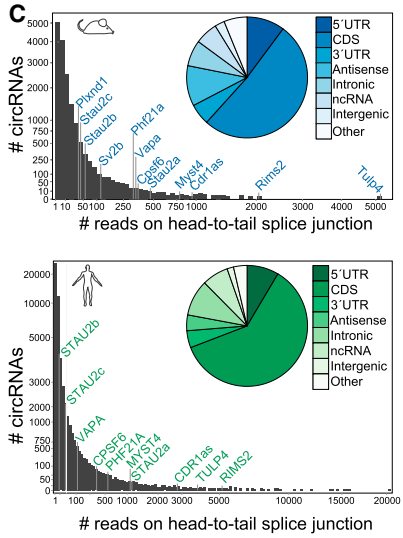

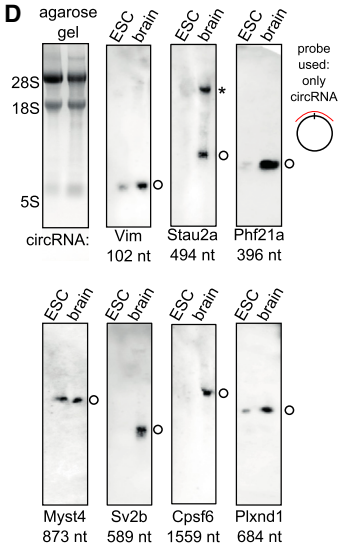

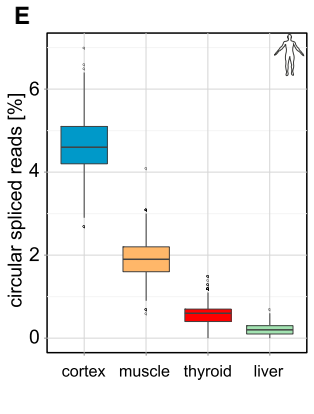

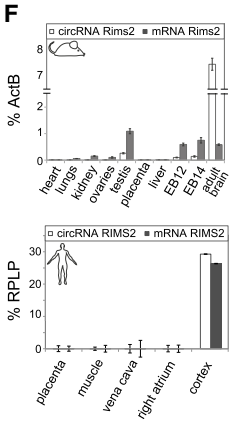

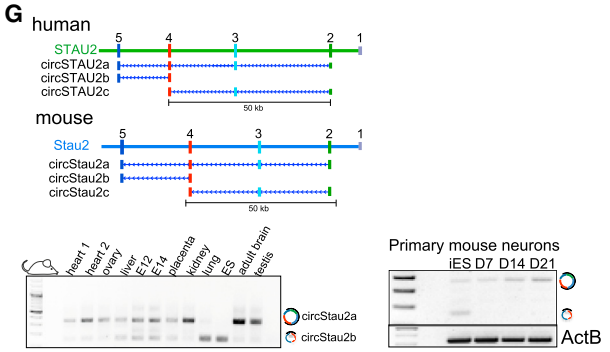

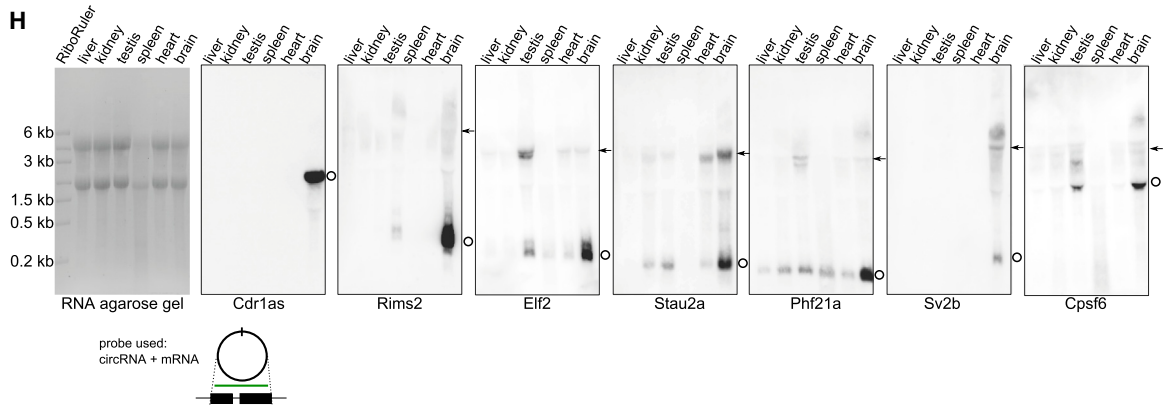

(legend on next page)

A striking example is the mouse circRNA generated from *Rims2*. In the adult brain, it is expressed ~20-fold higher than the linear mRNA, but is lowly expressed in other mouse tissues (see Experimental Procedures; Figures 1F, 1H, and S1H). This circRNA and its expression pattern are conserved in human (Figure 1F). Another example is two conserved circRNAs from the RNA-binding protein Staufen 2 gene (Figure 1G), which show differential expression among the analyzed tissues. While the longer circRNA isoform (containing exons 2–5) is expressed in the majority of adult mouse tissues, the shorter, consisting of exons 4 and 5, is predominantly expressed in embryonic stem (ES) cells, embryonic tissues, and lung (Figure 1G). We also observed reciprocal expression of these circRNAs during neuronal differentiation (Figure S1G), which suggests that circularization is a tightly regulated event in different tissues and during neuronal development.

The highly brain-specific expression of some circRNAs, despite more widespread expression of linear transcripts from the same gene, required independent testing. By northern blots, using probes detecting both linear and circular isoforms, we validated 7/7 circRNAs to be specifically enriched in the brain (Figure 1H), although their linear isoforms mostly show much broader expression patterns across tissues. Numerous circRNAs were found as the predominant isoform in brain (examples include circRims2, circTulp4, circElf2, circPhf21a, and circMyst4; Figures 1H and S1F).

circRNAs Are Differentially Expressed in the Brain

To obtain an overview of spatial circRNA expression patterns in the CNS, we clustered mouse circRNA expression data of different brain regions (olfactory bulb, prefrontal cortex, hippocampus, and cerebellum), normalized for sequencing depth (see Supplemental Computational Procedures). This revealed differential expression between brain regions, with an overall enrichment of circRNA expression in the cerebellum (Figure 2A). Interestingly, the ratio of circular to linear expression was also significantly higher in the cerebellum (Figure S2C). Since the cerebellum has a higher density of neuronal cells compared to other brain regions, the observed enrichment would be consistent with specifically high circRNA expression in neurons.

We tested the expression patterns of 13 circRNAs and their linear isoforms in six dissected mouse brain regions by qRT-PCR (Figure 2B). The already-characterized circRNA CDR1as served as a positive control. The majority of analyzed circRNAs followed the pattern of their linear isoform, but we found several circRNAs enriched in specific brain regions—independent of their linear isoforms. Some circRNAs were highly enriched in the cerebellum: circRims2, circElf2, and circDym, while circPlxnd1 was enriched in the cortex (Figure 2B). Moreover, we assayed the spatial expression patterns of four circRNAs by in situ hybridization using circRNA-specific (Figures S2A and S2B) short RNA probes on sagittal sections of adult mouse brain (Figure 2C). circRims2 was detected exclusively in the granular layer of the cerebellum. circElf2 and circPhf21a showed predominant expression in the granular layer of cerebellum and olfactory bulb, consistent with qRT-PCR and northern blot analysis (Figure 2C). The control, Cdr1as, showed the previously described expression pattern (Hansen et al., 2013; Memczak et al., 2013).

circRNAs Are Highly Enriched in Synapses

Many mRNAs are translated in the synapse in an activity-dependent fashion, which plays a role in synaptic plasticity (Bramham and Wells, 2007). Given their prevalence in the brain, we asked whether circRNAs are specifically present in synapses. We sequenced highly pure synaptoneurosome fractions (Figures S2D and S2E), corresponding cytoplasmic fractions, and adult mouse brain. We considered circRNAs with at least one splice site annotated in the Ensembl database (Cunningham et al., 2015), and at least five junction-spanning reads in one of the samples, and compared their expression between samples. This revealed that circRNAs are enriched in the synaptoneurosome (Figure 2D), which might indicate active transport of circRNAs to synapses. Moreover, by normalizing circRNA abundance to host gene expression (Figures 2E, S2F, and S2G; Table S3), we found that circRNAs are strongly enriched in synaptoneurosomes compared to the whole-brain lysate and cytoplasm on all expression cutoffs. Using independently prepared samples, we validated synaptic enrichment for 12/17 tested circRNAs. One example is the previously mentioned circStau2a, which localizes primarily to synapses, whereas the linear *Stau2*

Figure 1. circRNAs Are Highly Abundant in Mammalian Brain

(A) circRNAs were detected as previously described (Memczak et al., 2013), and the analysis was extended by a comparison of circRNA and host transcript expression in deep sequencing data ("Quantification module").

(B) A total of 29 CNS-related samples were analyzed for this study.

(C) circRNAs detected in mouse and human brain samples span a broad expression range and are mostly derived from the CDS. Mouse candidates validated in (D), (F), (G), and (H) were selected from the entire expression range, and their human orthologs roughly resemble the expression levels observed in mouse.

(D) circRNA expression in the mouse brain was validated by northern blots. *, unspecific band. The right panel shows probe design used for northern blot detection.

(E) From reads that were found to overlap splice junctions in four human sequencing libraries, the highest fraction was assigned to circular splice junctions in cortex (blue), compared to muscle (yellow), thyroid gland (red), and liver (green). Boxes are limited by the first quartile and the third quartile, median is indicated as a horizontal bar, while whiskers span 1.5 × inter-quartile range from their hinges. Outliers beyond the whiskers are plotted as points.

(F) The conserved circRims2 is highly expressed in mouse adult brain (upper panel; EB12/14, embryonic brain day 12/14; AB, adult brain) or human cortex (lower panel). Data are given as mean ± SD, n = 3 technical replicates.

(G) Three different circRNA isoforms are derived from Stau2 gene in human and mouse. Two of them show differential expression across mouse tissues. iES, induced mouse ES cells; D7/D14/D21, primary mouse neurons at days 7/14/21 post-plating.

(H) Northern blot analyses showing circRNA and linear mRNA transcript expression across mouse tissues. Arrows, linear transcripts; circles, circRNA. The lower panel shows a scheme of probe design.

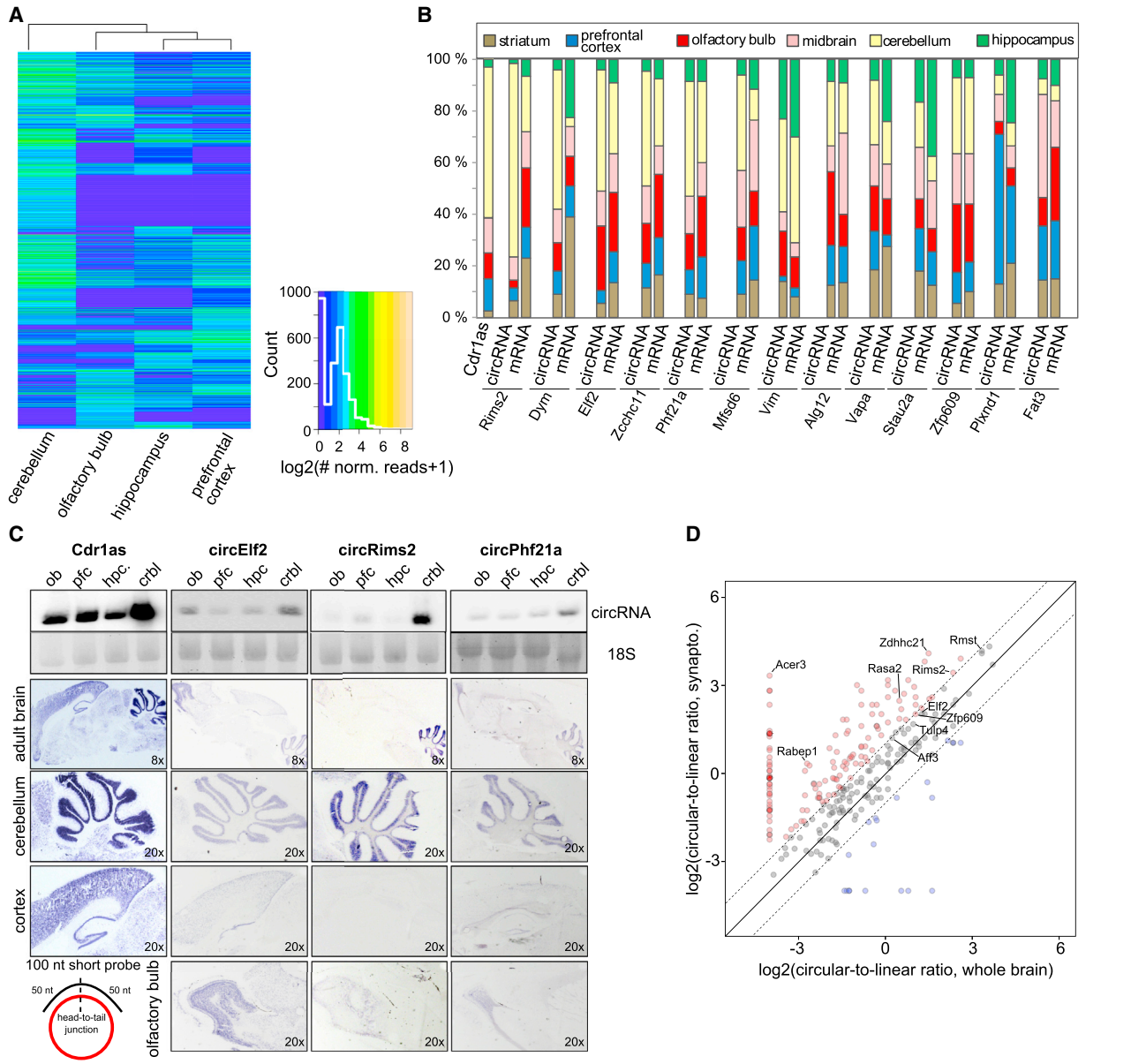

(legend on next page)

mRNA transcript is almost exclusively present in the cytoplasm. Perhaps even more striking is the very high synaptic enrichment of the circRNA from the nuclear lncRNA *Rmst*, a known regulator of neuronal differentiation (Ng et al., 2013). However, not all circRNAs localize to the synapse. CDR1as shows predominantly cytoplasmic localization (Figure 2F).

Together, our data reveal differential localization of linear and circular transcripts derived from the same gene and suggest that some circRNAs function at the synapse, independent of their corresponding linear transcripts.

circRNAs Are Differentially Expressed during Neuronal Differentiation

Given the high abundance of circRNAs in the mammalian brain, we asked if circularization could play a role in defining neuronal cell identity. We examined the expression changes of circRNAs during early neuronal cell specification using established cell culture models for neuronal development (McBurney, 1993; Monzo et al., 2012). Mouse P19 EC neuronal differentiation was induced by stimulation with retinoic acid, embryoid body (EB) formation, and subsequent Neurobasal/N2/B27 adherent culture (see Supplemental Experimental Procedures). Samples were collected at days 0, 2, and 4 of EB formation and finally at day 12 of neuronal culture. Human SH-SY5Y cells were assayed 4 days after retinoic acid treatment. Differentiated cells showed a neuronal characteristic with increased expression of neuronal markers (β-III-Tubulin, NeuroD1, NeuN), and almost no expression of the astrocytic marker GFAP (Figures S3A, S3B, S3E, and S3F). To capture in vivo processes such as axo-dendritic development and synapse formation, we additionally sequenced RNA from cultures of embryonic (E18) cortical neurons at days 1, 7, 14, and 21 after the initial plating.

In total, 2,735 circRNAs were detected in P19, as well as 4,264 in SH-SY5Y cells and 5,265 in primary cortical neurons (Tables S4, S5, and S6). From these, 238 were downregulated and 1,116 upregulated during P19 differentiation, as well as 797 and 1,926 during primary neuron maturation, respectively (Figures 3A and 3B). This overall induction of circRNAs indicates that circularization is not only accompanying neuronal commitment, but is also likely important for neuronal function, because many circRNAs are upregulated at different time points of neuronal maturation (Figures 3A–3D). Interestingly, we also observed that although circRNA upregulation was consistent between independent experiments (Table S4), the level of upregulation correlated with neuronal culture homogeneity and decreased with higher numbers of glia cells (GFAP-positive cells) in the culture. This implies that circRNA induction is specific for the neuronal, not glial, cells, and cannot be explained by accumulation in non-dividing cells.

Subsequently, the top differentially expressed circRNAs from P19 cells and primary neurons were selected for further validation and analysis. Many of these originate from protein coding genes with pivotal roles in neurons (e.g., synaptic membrane exocytosis, *Rims2*; dendritic mRNA transport, *Stau2*) or non-coding RNAs with already-described function in differentiation (*Rmst*). As shown in Figure S3C, the majority of tested circRNAs showed RNase R resistance, confirming circularity, while corresponding linear transcripts were efficiently depleted. Additionally, we confirmed the predicted head-to-tail junction sequences for many candidates by Sanger sequencing (Figures S3D, S1E, and S5C). Finally, using independent biological replicates, we validated the differential expression by qRT-PCR, showing that the circRNA expression changes inferred from sequencing data overall correlate with qRT-PCR measurements (Figures 3E and 3F).

Since undifferentiated SH-SY5Y cells resemble immature catecholaminergic neurons (Ross et al., 1983), the high number of circRNAs already expressed in uninduced cells (day 0) and overall less-prominent circRNA upregulation upon differentiation (day 4) (Figures 3G and 3H) are not surprising. However, we found many circRNAs upregulated during P19 differentiation to also be upregulated during human SH-SY5Y differentiation (Figure 3I), suggesting conservation of circRNA expression during neuronal differentiation. Some conserved candidates were validated (Figures S3G and S5C). Using mouse embryonic and postnatal brain developmental stages, we confirmed that circRNAs are also upregulated during mouse brain maturation in vivo, particularly during postnatal development, when synaptic connections and neuronal networks are established (Figure S3H).

circRNA and Linear mRNA Expression Changes Can Differ

It has been recently proposed that relative levels of circRNAs and linear transcripts from the same gene can differ between cell types (Salzman et al., 2013). An extreme example of this is the fly muscleblind circRNA, which is by far the most abundant RNA expressed from the *muscleblind* gene in fly heads, while in cell culture (S2 cells) the normal linear muscleblind mRNA is expressed much higher than the circular isoform (Ashwal-Fluss et al., 2014). Such instances indicate cell type-specific factors for degradation and/or production, which differentially affect the circular and linear products of a gene. To get an overview

Figure 2. circRNAs Are Differentially Expressed in Brain and Neuronal Compartments

(A–C) circRNAs show differential expression patterns across mouse brain regions.

(A) Clustering of mouse brain region samples by circRNA expression (normalized reads) in mouse brain regions.

(B) qRT-PCR analysis of circRNAs and linear isoform expression in mouse brain regions.

(C) In situ hybridization and northern blot analysis of circElf2, circRims2, and circPhf21a expression in adult mouse brain. Upper panel shows northern blot analyses of circRNA expression in the corresponding mouse brain in situ: ob, olfactory bulb; pfc, prefrontal cortex; hpc, hippocampus; crbl, cerebellum. 18S, loading control. The lower-left panel shows a scheme of probe design. Cdr1as, positive control.

(D) circRNAs are enriched in synaptoneurosomes compared to whole brain. Dashed line, 2-fold cutoff.

(E) The circRNA enrichment in synaptoneurosomes was observed throughout the expression range of circRNAs. Boxes are limited by the first quartile and the third quartile, median is indicated as a horizontal bar, while whiskers span 1.5 × inter-quartile range from their hinges. Outliers beyond the whiskers are plotted as points.

(F) qRT-PCR validation of differential circRNA localization. Data are given as mean ± SD, n = 3 technical replicates.

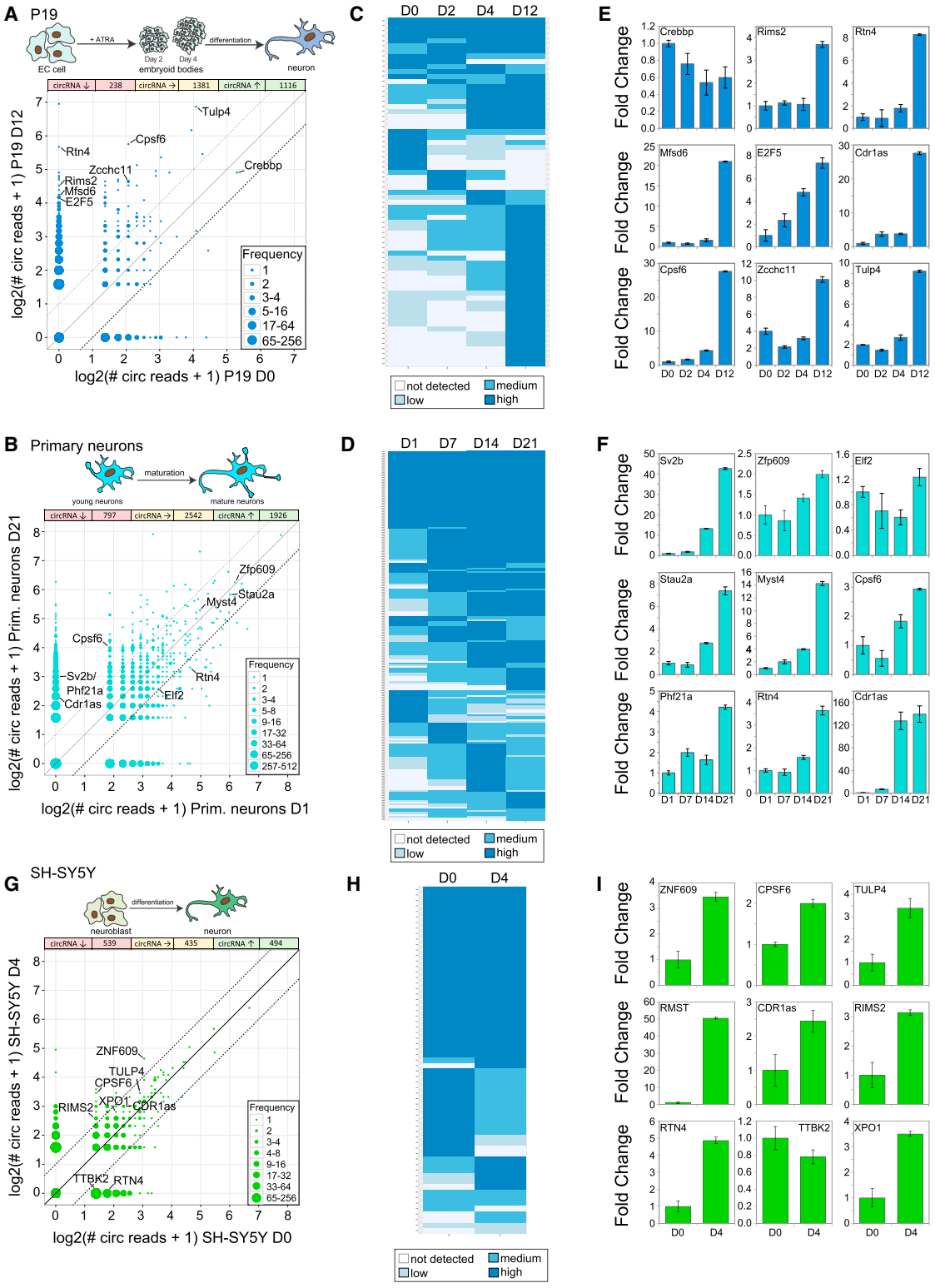

Figure 3. circRNAs Are Differentially Expressed during Neuronal Differentiation

(A–F) circRNA expression analysis during early neuronal differentiation and neuronal maturation.

(A) circRNA log2 fold changes between day 0 (D0) and day 12 (D12) of P19 cell differentiation.

(B) circRNA log2 fold changes between mouse embryonic neurons day 1 (D1) and mature neurons day 21 (D21). Dashed line, 2-fold cutoff.

(legend continued on next page)

of this phenomenon in our model systems for neuronal differentiation, we combined the circular-to-linear ratios (CLRs) from our quantification module with a standard measure for overall host gene mRNA expression, the transcripts per million (TPM). We note that our approach is conservative, since reads that belong to circRNAs will artificially increase the TPM values, as it is not possible to decouple the RNA-seq coverage signal on shared exons.

We observe a negative correlation between gene expression and the logarithm of the CLR at all time points (Figures 4A, 4D, and 4G; Figures S4A and S4B for intermediate time points). This argues against the idea that circRNAs are a by-product of occasional aberrant splicing, in which case we would expect no dependence of the CLR on total expression. Rather, we observe that overall, highly expressed genes give rise to relatively less circRNA.

However, upon neuronal development, the CLRs of many genes, from all expression levels, significantly increase (an effect that is most pronounced for synaptic fractions; Figure S4C). The scatter plots and summarizing tables in Figures 4B, 4C, 4E, 4F, 4H, and 4I show that while the expression changes of linear and circular transcripts during differentiation are overall correlated, there are many examples with differential changes of the two types of RNA produced from the same gene.

We selected several of the circRNAs, which showed a high CLR in at least one differentiation stage, and tested their expression changes with qRT-PCR and northern blots with independent biological replicates (Figures 4J–4L, S4D, and S4E). As seen from the sequencing data, many of the analyzed circRNAs increase when linear transcript expression also increases (*Rims2*, *Elf2*, *Mfsd6*, *Crebbp*), but rarely by the same factor. Interestingly, some circRNAs showed even a reciprocal expression pattern during differentiation (cleavage- and polyadenylation-specific factor *Cpsf6*, PHD finger protein *Phf21a*, or zinc finger *Zfp609*) (Figures 4J and 4K), which supports the previous finding that circularization can compete with linear splicing (Ashwal-Fluss et al., 2014).

The Expression of Neuronal circRNAs Is Conserved

Next, we analyzed if the expression of neuronal circRNAs is conserved between mammals. We used the liftOver tool (Hinrichs et al., 2006), which exploits whole-genome alignments, to find the orthologous coordinates for all mouse circRNA splice sites (see Supplemental Computational Procedures). We strictly defined the expression of a mouse circRNA as conserved if a human circRNA, independently observed to be circular in this study, had its splice sites within 2 nt, excluding even small shifts of a splice site position during 100 million years of evolution. By this definition, 4,522 out of 15,849 mouse circRNAs were conserved in humans (Table S1). Figure 5A shows a typical case, the conservation of the circRNA Tulp4. Conservation of circRNA expression increased with expression (Figure 5B). For another 4,527 mouse circRNAs we observed overlapping human circRNAs with one identical splice site and one different splice site. These events indicate that splice sites compete in circRNA biogenesis, and might be explained by the acquisition or loss of complementary elements in the surrounding introns. For 5,278 mouse circRNAs, no human homolog was detected, and for 1,522, we could not map the splice sites to the human genome. We selected 19 candidates with conserved expression for further validation (Figure S5A). We could confirm their circularity in human SH-SY5Y and mouse brain by RNase R treatment (Figure S5B). Moreover, by Sanger sequencing we found that the head-to-tail junction sequences are precisely conserved between human and mouse (Figure S5C).

Conservation of Intronic Sequences Flanking Conserved circRNAs

The conservation of circRNA expression between human and mouse suggests that their mechanism of biogenesis might also be conserved. Introns flanking a circRNA often contain reverse complementary matches (RCMs), which facilitate back-splicing of the enclosed circRNAs (Ashwal-Fluss et al., 2014; Liang and Wilusz, 2014; Ivanov et al., 2015; Starke et al., 2015). Recently, we developed the H-score, which can be used to quantify these inter-intronic interactions and to predict which exons will be circularized (Ivanov et al., 2015; Figure 5C). We calculated H-scores for all circRNAs detected in this study. This analysis reveals that the presence of RCMs in both human and mouse introns flanking a circRNA is clearly a hallmark of circRNAs with conserved expression (Figure 5D). We note that very often these RCMs are repetitive elements, which evolve quickly in time. Thus, multiple species alignments of such RCMs are often poor.

Highly Expressed circRNAs Contain Well-Conserved Sequences

Conservation of circularization indicates that selection acts to preserve the conditions in which the splicing machinery circularizes specific exons. This could be due to *cis*-effects on the splicing of the linear mRNA or due to independent functions of circRNAs. In the latter case, circRNA sequences would be under additional selection. As most circRNAs are derived from coding (CDS) exons, we focused on circRNAs that fall entirely into the CDS, such that the adjacent segments of the CDS, before and after the circRNA, were available as controls (Figure 6A). We further binned these segments on the expression level of the circRNAs. In each group of segments we counted the conserved occurrences of 7-mer sequences in the branch of the vertebrate phylogeny that spans from human to chicken

(C and D) Heatmap comparisons.
(C) P19 differentiation time points (D0, undifferentiated cells; D2/D4, embryoid bodies days 2/4; D12, neurons day 12).
(D) Neuronal maturation time points at days 1, 7, 14, and 21 post-plating.
(E and F) qRT-PCR validation of circRNA expression during P19 differentiation (E) and primary neurons maturation (F).
(G and H) circRNAs are differentially expressed during induction of human SH-SY5Y cells to neurons. Log2 fold changes (G) and heatmap (H) comparison between day 0 (D0) and day 4 (D4) of SH-SY5Y differentiation.
(I) qRT-PCR validation of circRNA expression in SH-SY5Y cells. Data in (E), (F), and (I) are presented as mean ± SD, n = 3 technical replicates.

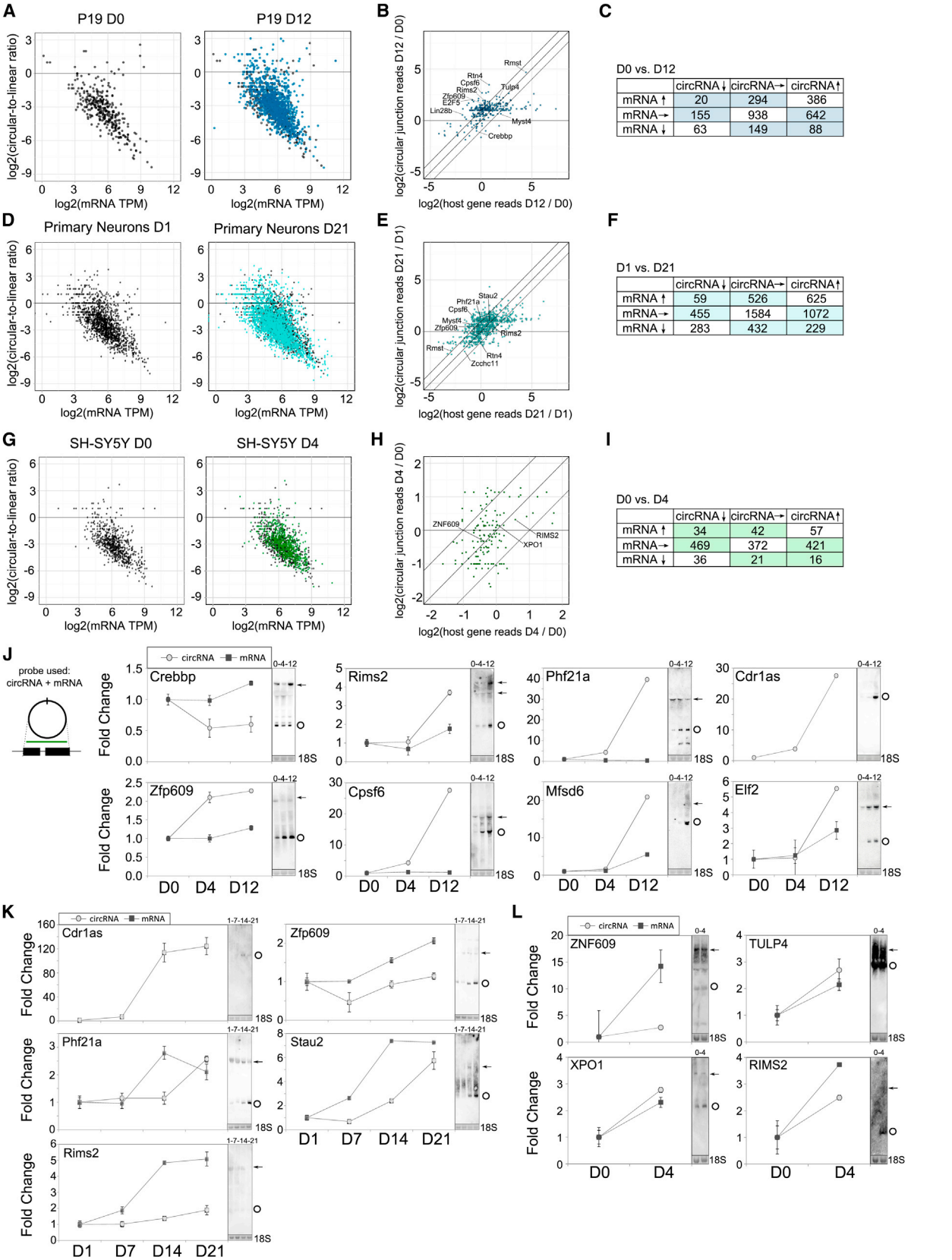

(legend on next page)

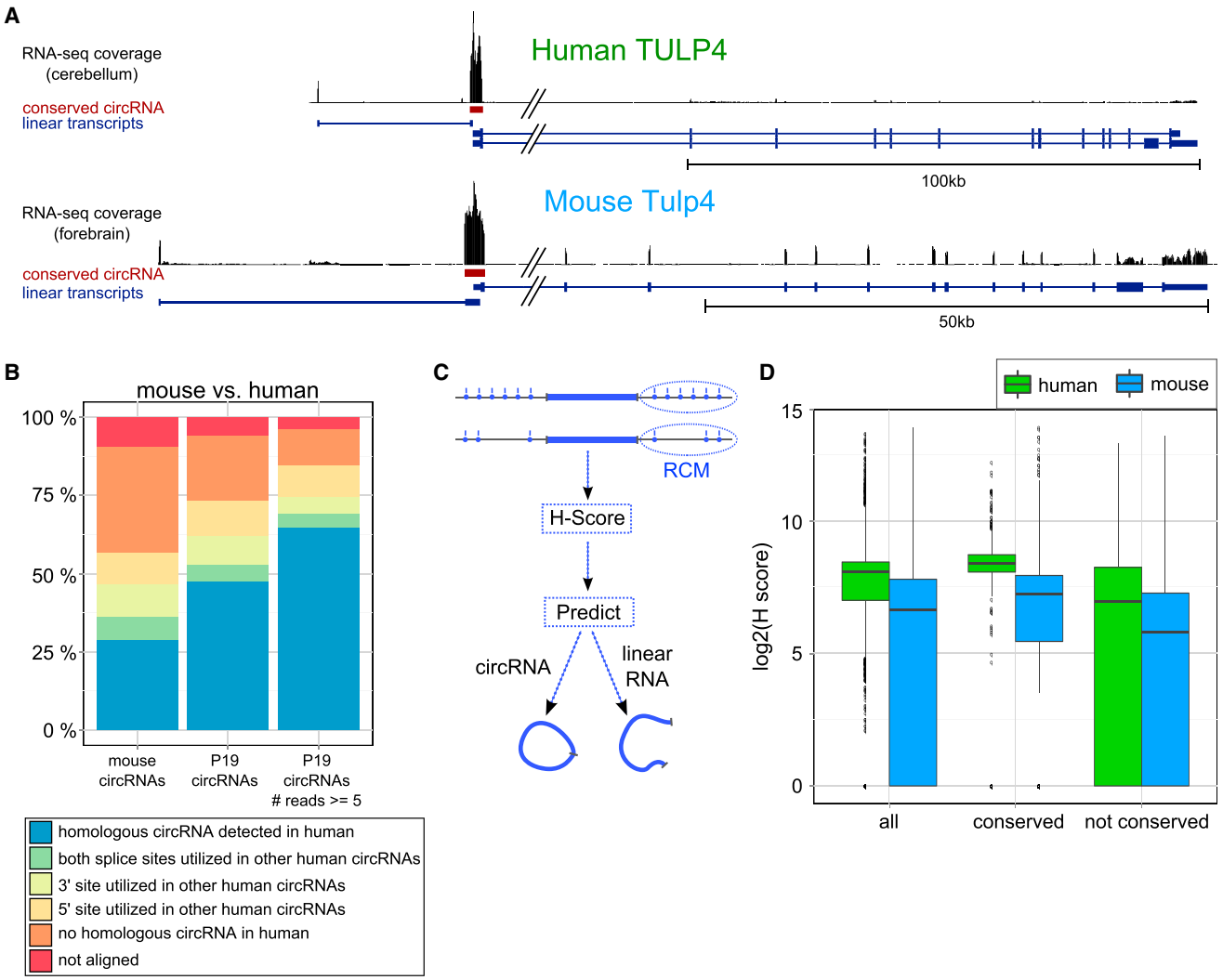

Figure 5. circRNAs Are Conserved

(A) Ribominus sequencing coverage (black) from human cerebellum and mouse forebrain for Tulp4 gene (blue) and circRNAs (brown). The conserved circTulp4 isoform is spliced from the homologous exons in human and mouse, and shows similar relative expression compared to the surrounding (non-circularized) exons.

(B) Conservation analysis for circRNAs in human and mouse reveals that highly expressed mouse circRNAs are more likely to be conserved in human.

(C) The H-score is a measure for circularization probability (see Supplemental Computational Methods).

(D) circRNAs conserved between mouse and human show higher circularization probability, based on the H-score, in both organisms. Boxes are limited by the first quartile and the third quartile, median is indicated as a horizontal bar, while whiskers span 1.5 × inter-quartile range from their hinges. Outliers beyond the whiskers are plotted as points.

and recorded the length of the corresponding segments. By this analysis we find a significantly higher mean density of conserved 7-mers inside circRNAs compared to the flanking parts of the CDS (Figure 6B; Supplemental Computational Procedures). The density furthermore increases with higher circRNA expression. The phyloP score (Pollard et al., 2010) for vertebrate conservation confirms the elevated conservation of circRNAs (Figure S6A). However, here the effects are weaker,

Figure 4. circRNA and mRNA Expression Changes Differ

(A–I) Relative quantification of circRNA expression during differentiation of P19 cells (A–C), primary neurons (D–F), and SH-SY5Y cells (G–I). Circular-to-linear ratio plotted against host gene TPM shows that circRNA production rate is not constant throughout the gene expression range, and that many circRNAs are expressed higher than their linear counterparts (A, D, and G). circRNAs' expression change between initial and final stages of differentiation is positively correlated with the expression change of host genes, but many exemptions were observed in all three differentiation systems (B, E, and H). The summary of circRNA/host gene expression changes is given in (C), (F), and (I).

(J–L) qRT-PCR and northern blot validation of differential circRNA expression during P19 (J), primary mouse neuron (K), and SH-SY5Y (L) cell differentiation. Data are shown as mean ± SD, n = 3 technical replicates.

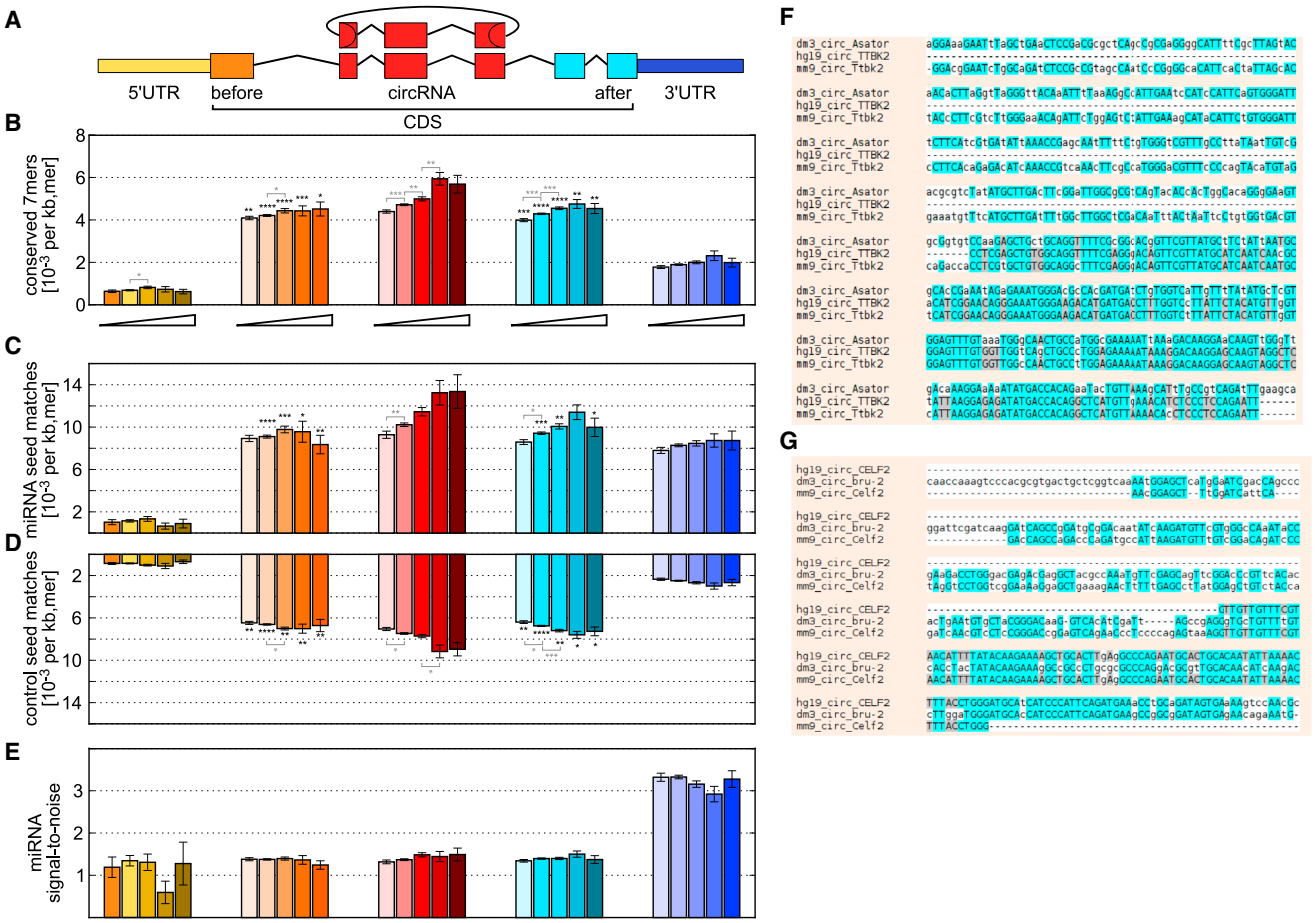

Figure 6. Sequence Conservation of circRNAs

(A) Intersection of circRNAs with known transcripts yields up to three segments of CDS. Orange, 5′ of circRNA; red, part of circRNA; light blue, 3′ of circRNA. 5′ UTRs (yellow) and 3′ UTRs (blue) were used as control.

(B) Bar plots show the mean density (total number of occurrences per total spliced length) of 7-mer sequences conserved up to chicken, in the sets of CDS segments sketched in (A), further subdivided by the expression level of the circRNA and normalized to the number of possible 7-mers. Ramp underneath indicates circRNA expression level, from left to right: 2–10, 10–100, 100–500, 500–1,000, 1,000+ head-to-tail-spliced reads. Error bars represent SD of the mean based on 1,000 random subsamples of half of the data. Asterisk symbols indicate significantly higher densities within circRNAs compared to the matched upstream/downstream CDS segments. *p < 5%, **p < 1%, ***p < 0.1%, and ****p < 0.01%.

(C and D) Bar plots analogous to (B), but for seed matches to 58 conserved vertebrate miRNAs (C) and shuffled, non-miRNA seed matches (D). For easier comparison, see (D) with inverted y axis.

(E) Ratio of conserved miRNA seed match occurrences and non-miRNA controls.

(F) Parts of the multiple species alignment of a deeply conserved circRNA. Exonic sequences of the *D. melanogaster* gene Asator are expressed as circRNA, as are the homologous exons of mouse Ttbk2 and human TTBK2. Nucleotides identical in 2/3 species are highlighted in gray, and identical in 3/3 are highlighted in blue.

(G) Similar to (F), but for the deeply conserved splicing regulator Bruli/Celf2.

probably because phyloP scores only individual nucleotides. We caution that the interpretation of this result is not straightforward because more highly expressed circRNAs generally derive from exons that are located closer to the transcription start of the host gene (Figure S6B), and CDS conservation is not homogeneous along the CDS (Figure S6C). More highly expressed circRNAs are also flanked by longer introns (Figure S6D), which correlate with elevated conservation levels of the exons (Figure S6E). We therefore specifically restricted our analysis to the 7-mer seed matches (pos. 2–9) of 58 miRNAs that are conserved among vertebrates (Krek et al., 2005) (Figure 6C). We repeated the analysis with 400 shuffled, non-miRNA control 7-mers that are matched for the frequency distribution of the real miRNA seed matches in 3′ UTRs (Figure 6D). Both sets show elevated densities of conserved occurrences within circRNA coding exons. However, the ratio between them (signal-to-noise ratio, compare Krek et al., 2005) does not differ from flanking CDS (Figure 6E). Here, 3′ UTRs serve as a positive control and show ~3-fold enrichment for conserved miRNA binding, consistent with previous studies (Krek et al., 2005). Analogous analyses of 6-mers and 8-mers were consistent with these results (data not shown).

We conclude that there is elevated sequence conservation in circularized CDS exons, compared to the remaining CDS.

However, we cannot conclude that this is due to selection on miRNA seed matches.

Some Mammalian Brain circRNAs Are Also Detected as circRNAs in Fly Brains

We used BLAST to find homologous sequences between the fruit fly, mouse, and human circRNAs (Supplemental Computational Procedures). Over such large evolutionary distances, exon-intron structures are often changed, and it is difficult to construct a null hypothesis for the expected number of homologous circRNAs. Nonetheless, we were able to trace some clear examples of homologous sequences being circularized in these vastly diverged organisms. Figures 6F and 6G show multiple species alignments of the conserved Tau-Tubulin kinase (*TTBK2,Ttbk2*, *Asator* in fly) and the ancient splicing regulator Bruli (*CELF2*/*Celf2* in human/mouse, *bru-2* in fly). The expression of these circRNAs in human, mouse, and *Drosophila* was validated (data not shown).

ADAR Expression Negatively Correlates with circRNA Levels in Neural Tissue in Flies and Mammals

The RNA-editing enzyme ADAR1 has been recently implicated in circRNA biogenesis by editing or hyper-editing of introns flanking circRNAs (Ivanov et al., 2015). Knockdown of ADAR1 significantly upregulates circRNA expression in human HEK293 cells (Ivanov et al., 2015). Moreover, Rechavi and co-workers showed editing levels within non-coding regions in undifferentiated human ES cells (hESCs) decrease when hESCs undergo differentiation (Osenberg et al., 2010). Therefore, we asked if ADAR1 could regulate circRNA biogenesis during cellular differentiation. We monitored ADAR1 levels during retinoic acid induction of mouse P19 EC and human SH-SY5Y cells, at the time points when circRNA upregulation was observed (Figures 7A and 7B). The short isoform of ADAR1 (p110) was the predominant isoform (Figures 7A and 7B) and decreased slightly to ~50% during neuronal differentiation, while the longer, lowly abundant isoform (p150) slightly increased in P19, but not in SH-SY5Y cells (Figures 7A and 7B). We depleted ADAR1 in mouse P19 and human SH-SY5Y cells to test its effect on circRNA expression (Figures S7A and S7B). We monitored the knockdown efficacy by western blotting and qRT-PCR (Figures S7A–S7D, 7C, and 7D). The expression of 9/15 mouse circRNAs (Figure 7C) and 8/10 human circRNAs (Figure 7D) increased upon ADAR1 depletion (Figure 7D). For 4/9 upregulated mouse circRNAs (4/8 for human) this is not accompanied by a corresponding increase in linear mRNA expression (Figures S7C and S7D).

Additionally, we observed changes in the editing activity in the flanking introns of the upregulated circRTN4 (Figure 7E). Here, editing decreases between D0 and D4, but is restored at D8. Consistent with an intermittent increase in the rate of circRNA production, circRTN4 concordantly increases between D0 and D4.

To investigate whether the connection between editing and circRNA biogenesis in the nervous system is conserved through evolution, we turned to *Drosophila*. Editing by dADAR is regulated by temperature in *Drosophila* (Rieder et al., 2015; Savva et al., 2012). We compared the expression levels of circRNAs in fly heads maintained at 18°C and 29°C for 3 days (previously published dataset, Ashwal-Fluss et al., 2014). We observed a strong and significant increase in circularization at 29°C compared to 18°C (Figures 7F and 7G), but not in linear isoform expression (Figures S7E and S7F). The effect of temperature on circRNA biogenesis was independent of the elongation rate of RNA-Pol II as we observed a similar effect in C4 (slow polymerase) flies (data not shown). Although we cannot determine if this is due to a direct alteration in editing or a change in RNA secondary structure affecting the circularization and/or ADAR binding, these data taken together suggest a conserved regulation of circularization related to ADAR activity.

DISCUSSION

In this study, our comprehensive sequencing and analysis of ribosomal-depleted RNA from 29 different types or stages of neural cells and tissues has revealed high and specific expression of circRNAs in the brain. Expression is often specific to different brain compartments. The olfactory bulb, prefrontal cortex, hippocampus, and cerebellum all produce specific sets of highly expressed circRNAs (Figure 2A). Interestingly, our study strongly suggests that circRNAs are not equally distributed in the neuronal compartments, but are highly enriched in the synapses. This could be one of the reasons why we observe higher numbers of circRNAs in human compared to mouse brain, because synaptic density in the human cerebral cortex may be four times higher than in the mouse brain (Herculano-Houzel, 2009). Another possible reason could be the expanded repertoire of inverted Alu repeats in primate introns (Daniel et al., 2014). We observed that circRNA expression increases during neuronal differentiation, both in cell line systems and in primary neuron culture. This increase in circRNA expression during neuronal differentiation was often coupled to upregulation of the linear host transcripts. However, we observed many notable exceptions. For example, circStau2a and circStau2b, expressed from RNA-binding protein Staufen 2 (Figure 1G), have distinct expression patterns in ES cells and other assayed neural samples, and display inverse expression changes during neuronal maturation. Another example is circZfp609. Its mRNA is expressed on a constant level during neuronal differentiation, while the circRNA is highly upregulated in neurons. We note that the specific expression of circRNAs and their stability make them very interesting candidates as biomarkers for neurodegenerative diseases, such as Alzheimer's disease. In support of this finding is a recent report on downregulation of CDR1as in Alzheimer's patients (Lukiw, 2013).

What regulates the specific expression of circRNAs? Splice regulators such as muscleblind have been linked to circRNA biogenesis (Ashwal-Fluss et al., 2014) as well as the RNA-binding protein QKI (Conn et al., 2015), demonstrating that *trans*-acting factors can explain at least some of the observed expression patterns. Recently, ADAR1 has been suggested as an antagonist of circRNA production (Ivanov et al., 2015). Our data are consistent with this finding. ADAR1 knockdown caused upregulation of circRNAs (Figures 7C and 7D) in cell line systems, and also in *Drosophila*, where editing depends on temperature. It will be interesting to understand how circRNAs can be highly expressed in neurons or during development where ADAR1 is known to have a high activity (Wahlstedt et al., 2009). ADAR1 may be in competition with circRNA-promoting factors, such as muscleblind.

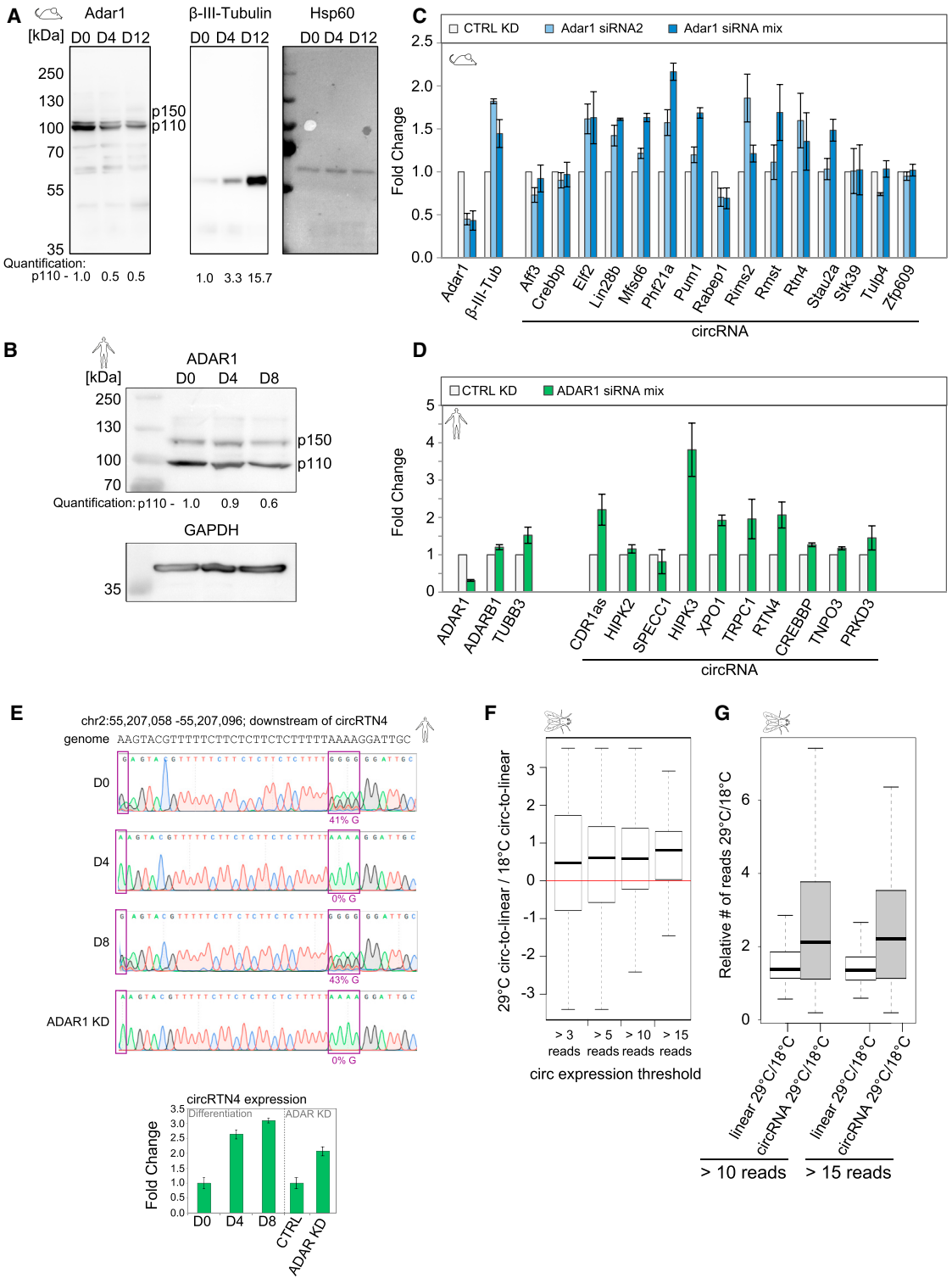

Figure 7. ADAR and circRNAs

(A and B) ADAR1 expression decreases during P19 (A) and SH-SY5Y (B) cell differentiation. Hsp60 and GAPDH, loading controls; β-III-Tub, neuronal marker.

(C and D) circRNA expression upon knockdown of Adar1 in P19 (C) and SH-SY5Y cells (D). Corresponding mRNA expression in Figures S7C and S7D. Data are given as mean ± SD, n = 3 biological replicates.

(E) A-to-I editing by ADAR1 causes nucleotide A to be read as G in Sanger sequencing of the region in the flanking intron of circRTN4. Editing highlighted by purple box. Average fraction of nucleotide G intensity underneath. Editing levels anti-correlate with circRTN4 expression changes.

(legend continued on next page)

We were surprised by the high conservation of circRNA expression. Most well-expressed circRNAs in mouse were also present as circRNAs in human. Conserved circRNAs were more likely to be flanked by introns with RCMs than non-conserved ones. Neuronal genes often have long (> 10 kb) introns, and the length of these introns is highly conserved in evolution. One possible reason might be conserved expression of circRNAs, which have a high chance to be flanked by long introns (Jeck et al., 2013; Ivanov et al., 2015). However, it could be that introns in these genes are long for other reasons, and that circRNA production is a by-product of the complex splicing ("recursive splicing"; Burnette et al., 2005).

Likewise, the elevated conservation within circRNA sequences could be explained in different ways. It could indicate additional functions, independent of the open reading frame; for example, binding to RNA-binding proteins or miRNAs. This would certainly differ between circRNAs and is therefore hard to pinpoint by statistical analysis of the entire set of circRNAs. Alternatively, it could reflect constraints on exons that are flanked by long introns, imposed by the splicing machinery to achieve proper exon definition. Lastly, if circRNAs can be translated, it may also reflect the elevated selection pressure on highly expressed protein sequences. In any event, our conservation analyses make a strong case that production of circRNAs is functionally important, and that circRNAs' primary sequences are functionally important.

What could be the functions of circRNAs in the mammalian brain? Because of their stability, circRNAs could serve as topologically complex platforms to assemble RNP granules or to transport proteins or RNAs. The pronounced localization of many circRNAs to the synapse, which is often in contrast to the cytoplasmic localization of the corresponding mRNAs, points in this direction. We note that miRNAs can cleave circRNAs (Hansen et al., 2011), and therefore cargo "release" mechanisms are straightforward to imagine. Finally, due to their high stability, circRNAs might be used by neuronal termini and molecular postsynaptic platforms as synaptic tags to keep a molecular memory.

EXPERIMENTAL PROCEDURES

Cell Lines

Maintenance and neural induction of P19 and SH-SY5Y cells followed established protocols (Supplemental Experimental Procedures). Primary forebrain neurons were prepared from CD1 mouse embryos (E17.5–E18.5) as previously described (Supplemental Experimental Procedures). All animals used in this study were handled and sacrificed in accordance with German institutional regulations.

Synaptoneurosome Preparation

Synaptoneurosomes were isolated with some modifications as previously described (Supplemental Experimental Procedures).

Preparation of RNA-Seq Libraries

RNA spiked with ERCC RNA Spike (Life Technologies) was depleted of rRNA using the RiboMinus Kit v2 (Life Technologies). cDNA libraries were generated according to the Illumina TruSeq RNA-seq protocol and sequenced on an Illumina HiSeq 2000 in 1× 100 cycle runs (Supplemental Experimental Procedures).

Northern Blots of Agarose Gel

RNA denatured in Glyoxal Loading Dye (Ambion) was resolved on agarose gels and transferred to a Hybond-N+ membrane (GE Healthcare). Membranes were crosslinked, pre-hybridized (NorthernMax, Roche), and hybridized with in vitro-transcribed DIG-labeled probes. Stringent washing of the membranes was followed by incubation with anti-DIG AP-conjugated antibodies and visualization with CDP-Star Reagent (Roche) by LAS 4000 detection system (Supplemental Experimental Procedures).

In Situ Hybridization of Mouse Brain on Mouse Brain Sections

In situ hybridization was performed on mouse brain sagittal cryosections using short in vitro-transcribed, DIG-labeled probes spanning head-to-tail junctions. Specific hybridization signals were visualized using BCIP/NBT substrates (Supplemental Experimental Procedures).

RNA Isolation and qRT-PCR

Total RNA was extracted using TRIzol (Invitrogen). qRT-PCR reactions were performed on a 96-well format Applied Biosystems real-time PCR machine using SYBR green dye (Fermentas) according to the manufacturer's protocols (Supplemental Experimental Procedures).

Primers

All primers, listed in Table S7, were designed using the Primer 3 tool.

Computational Analysis

All computational methods are described in the Supplemental Computational Procedures.

ACCESSION NUMBERS

The accession number for the sequencing data reported in this paper is GEO: GSE65926.

SUPPLEMENTAL INFORMATION

Supplemental Information includes seven figures, seven tables, Supplemental Experimental Procedures, and Supplemental Computational Procedures and can be found with this article online at http://dx.doi.org/10.1016/j.molcel.2015.03.027.

AUTHOR CONTRIBUTIONS

A.R.-W. and C.S. performed all the experimental validation assays with the help of M. Herzog and L.S. P.G. performed the majority of computational analyses, except conservation (M.J.), clustering (P.P.), and intronic sequences conservation (A.I.) analyses. M.B. prepared synaptoneurosomes fractions; N.P. and S.G. prepared primary neuron samples. M. Hanan and O.B. performed *Drosophila* experiments, and R.A.-F. analyzed the *Drosophila* data. N.R., A.R.-W., C.S., P.G., and M.J. analyzed the data and wrote the paper with input from M.Ö., S.K., and D.R.

ACKNOWLEDGMENTS

The authors would like to thank all members of the N.R. lab for discussion and support. We would like to thank Anne von Euler and Neus Visa for the electron microscopy picture. Gregory Wulczyn's lab provided RNA from mouse developmental stages, Thomas Müller from Carmen Birchmeier's lab provided mouse embryonic brains, and Friedrich Luft's lab provided RNA from human

(F and G) Decreased dADAR activity in *Drosophila* observed at 29°C correlates with elevated exon circularization. The level of the hosting genes, as determined by linear splicing at the circRNA junction, is not significantly changed. Presented are circRNAs supported by at least 10 reads (n = 137) or 15 reads (n = 78). Boxes are limited by the first quartile and the third quartile, median is indicated as a horizontal bar, while whiskers span 1.5 × inter-quartile range from their hinges.

tissues. Robin Graf (Klaus Rajewsky lab) provided WT mouse brains for validation experiments, and Ami Citri provided mouse brains for sequencing. We thank the Erez Levanon lab for help with ADAR1 editing detection. We thank Claudia Langnick and Mirjam Feldkamp (Wei Chen lab, MDC) for performing sequencing runs. C.S. received a fellowship of the Boehringer Ingelheim Fonds. A.R.-W. was funded by a BIH-CRG 2a TP7 grant, P.G. by DEEP – German Epigenome Programme, M.J. by DFG RA 838/8-1, A.I. by GIF – German Israeli Foundation, and P.P. by the MDC/BIMSB-NYU PhD Exchange Program. S.K. was funded by a European Research Council Starting Grant (ERC #260911) and an Israel Science Foundation Grant (#814/2014) D.R. received grants from the Volkswagen Foundation and Max Planck Gesellschaft. N.R. received a BIH-CRG 2a TP7 grant.

Received: December 22, 2014
Revised: March 3, 2015
Accepted: March 20, 2015
Published: April 23, 2015

REFERENCES

Ashwal-Fluss, R., Meyer, M., Pamudurti, N.R., Ivanov, A., Bartok, O., Hanan, M., Evantal, N., Memczak, S., Rajewsky, N., and Kadener, S. (2014). circRNA biogenesis competes with pre-mRNA splicing. Mol. Cell *56*, 55–66.

Bernstein, B.E., Birney, E., Dunham, I., Green, E.D., Gunter, C., and Snyder, M.; ENCODE Project Consortium (2012). An integrated encyclopedia of DNA elements in the human genome. Nature *489*, 57–74.

Bramham, C.R., and Wells, D.G. (2007). Dendritic mRNA: transport, translation and function. Nat. Rev. Neurosci. *8*, 776–789.

Burnette, J.M., Miyamoto-Sato, E., Schaub, M.A., Conklin, J., and Lopez, A.J. (2005). Subdivision of large introns in *Drosophila* by recursive splicing at nonexonic elements. Genetics *170*, 661–674.

Capel, B., Swain, A., Nicolis, S., Hacker, A., Walter, M., Koopman, P., Goodfellow, P., and Lovell-Badge, R. (1993). Circular transcripts of the testis-determining gene Sry in adult mouse testis. Cell *73*, 1019–1030.

Conn, S.J., Pillman, K.A., Toubia, J., Conn, V.M., Salmanidis, M., Phillips, C.A., Roslan, S., Schreiber, A.W., Gregory, P.A., and Goodall, G.J. (2015). The RNA binding protein Quaking regulates formation of circRNAs. Cell *160*, 1125–1134.

Cunningham, F., Amode, M.R., Barrell, D., Beal, K., Billis, K., Brent, S., Carvalho-Silva, D., Clapham, P., Coates, G., Fitzgerald, S., et al. (2015). Ensembl 2015. Nucleic Acids Res. *43*, D662–D669.

Daniel, C., Silberberg, G., Behm, M., and Öhman, M. (2014). Alu elements shape the primate transcriptome by *cis*-regulation of RNA editing. Genome Biol. *15*, R28.

Dubin, R.A., Kazmi, M.A., and Ostrer, H. (1995). Inverted repeats are necessary for circularization of the mouse testis Sry transcript. Gene *167*, 245–248.

Glažar, P., Papavasileiou, P., and Rajewsky, N. (2014). circBase: a database for circular RNAs. RNA *20*, 1666–1670.

Gray, E.G., and Whittaker, V.P. (1960). The isolation of synaptic vesicles from the central nervous system. J. Physiol. *153*, 35–37.

Hansen, T.B., Wiklund, E.D., Bramsen, J.B., Villadsen, S.B., Statham, A.L., Clark, S.J., and Kjems, J. (2011). miRNA-dependent gene silencing involving Ago2-mediated cleavage of a circular antisense RNA. EMBO J. *30*, 4414–4422.

Hansen, T.B., Jensen, T.I., Clausen, B.H., Bramsen, J.B., Finsen, B., Damgaard, C.K., and Kjems, J. (2013). Natural RNA circles function as efficient microRNA sponges. Nature *495*, 384–388.

Herculano-Houzel, S. (2009). The human brain in numbers: a linearly scaled-up primate brain. Front. Hum. Neurosci. *3*, 31.

Hinrichs, A.S., Karolchik, D., Baertsch, R., Barber, G.P., Bejerano, G., Clawson, H., Diekhans, M., Furey, T.S., Harte, R.A., Hsu, F., et al. (2006). The UCSC Genome Browser Database: update 2006. Nucleic Acids Res. *34*, D590–D598.

Huttner, W.B., Schiebler, W., Greengard, P., and De Camilli, P. (1983). Synapsin I (protein I), a nerve terminal-specific phosphoprotein. III. Its association with synaptic vesicles studied in a highly purified synaptic vesicle preparation. J. Cell Biol. *96*, 1374–1388.

Ivanov, A., Memczak, S., Wyler, E., Torti, F., Porath, H.T., Orejuela, M.R., Piechotta, M., Levanon, E.Y., Landthaler, M., Dieterich, C., and Rajewsky, N. (2015). Analysis of intron sequences reveals hallmarks of circular RNA biogenesis in animals. Cell Rep. *10*, 170–177.

Jeck, W.R., and Sharpless, N.E. (2014). Detecting and characterizing circular RNAs. Nat. Biotechnol. *32*, 453–461.

Jeck, W.R., Sorrentino, J.A., Wang, K., Slevin, M.K., Burd, C.E., Liu, J., Marzluff, W.F., and Sharpless, N.E. (2013). Circular RNAs are abundant, conserved, and associated with ALU repeats. RNA *19*, 141–157.

Krek, A., Grün, D., Poy, M.N., Wolf, R., Rosenberg, L., Epstein, E.J., MacMenamin, P., da Piedade, I., Gunsalus, K.C., Stoffel, M., and Rajewsky, N. (2005). Combinatorial microRNA target predictions. Nat. Genet. *37*, 495–500.

Lasda, E., and Parker, R. (2014). Circular RNAs: diversity of form and function. RNA *20*, 1829–1842.

Liang, D., and Wilusz, J.E. (2014). Short intronic repeat sequences facilitate circular RNA production. Genes Dev. *28*, 2233–2247.

Lukiw, W.J. (2013). Circular RNA (circRNA) in Alzheimer's disease (AD). Front. Genet. *4*, 307.

McBurney, M.W. (1993). P19 embryonal carcinoma cells. Int. J. Dev. Biol. *37*, 135–140.

Memczak, S., Jens, M., Elefsinioti, A., Torti, F., Krueger, J., Rybak, A., Maier, L., Mackowiak, S.D., Gregersen, L.H., Munschauer, M., et al. (2013). Circular RNAs are a large class of animal RNAs with regulatory potency. Nature *495*, 333–338.

Monzo, H.J., Park, T.I.H., Montgomery, J.M., Faull, R.L.M., Dragunow, M., and Curtis, M.A. (2012). A method for generating high-yield enriched neuronal cultures from P19 embryonal carcinoma cells. J. Neurosci. Methods *204*, 87–103.

Ng, S.-Y., Bogu, G.K., Soh, B.S., and Stanton, L.W. (2013). The long noncoding RNA RMST interacts with SOX2 to regulate neurogenesis. Mol. Cell *51*, 349–359.

Osenberg, S., Paz Yaacov, N., Safran, M., Moshkovitz, S., Shtrichman, R., Sherf, O., Jacob-Hirsch, J., Keshet, G., Amariglio, N., Itskovitz-Eldor, J., and Rechavi, G. (2010). Alu sequences in undifferentiated human embryonic stem cells display high levels of A-to-I RNA editing. PLoS ONE *5*, e11173.

Pollard, K.S., Hubisz, M.J., Rosenbloom, K.R., and Siepel, A. (2010). Detection of nonneutral substitution rates on mammalian phylogenies. Genome Res. *20*, 110–121.

Rieder, L.E., Savva, Y.A., Reyna, M.A., Chang, Y.J., Dorsky, J.S., Rezaei, A., and Reenan, R.A. (2015). Dynamic response of RNA editing to temperature in *Drosophila*. BMC Biol. *13*, 1.

Ross, R.A., Spengler, B.A., and Biedler, J.L. (1983). Coordinate morphological and biochemical interconversion of human neuroblastoma cells. J. Natl. Cancer Inst. *71*, 741–747.

Salzman, J., Gawad, C., Wang, P.L., Lacayo, N., and Brown, P.O. (2012). Circular RNAs are the predominant transcript isoform from hundreds of human genes in diverse cell types. PLoS ONE *7*, e30733.

Salzman, J., Chen, R.E., Olsen, M.N., Wang, P.L., and Brown, P.O. (2013). Cell-type specific features of circular RNA expression. PLoS Genet. *9*, e1003777.

Savva, Y.A., Jepson, J.E.C., Sahin, A., Sugden, A.U., Dorsky, J.S., Alpert, L., Lawrence, C., and Reenan, R.A. (2012). Auto-regulatory RNA editing fine-tunes mRNA re-coding and complex behaviour in *Drosophila*. Nat. Commun. *3*, 790.

Shtrichman, R., Germanguz, I., Mandel, R., Ziskind, A., Nahor, I., Safran, M., Osenberg, S., Sherf, O., Rechavi, G., and Itskovitz-Eldor, J. (2012). Altered A-to-I RNA editing in human embryogenesis. PLoS ONE *7*, e41576.

Starke, S., Jost, I., Rossbach, O., Schneider, T., Schreiner, S., Hung, L.H., and Bindereif, A. (2015). Exon circularization requires canonical splice signals. Cell Rep. *10*, 103–111.

Wahlstedt, H., Daniel, C., Enstero, M., and Ohman, M. (2009). Large-scale mRNA sequencing determines global regulation of RNA editing during brain development. Genome Res. *19*, 978–986.

Westholm, J.O., Miura, P., Olson, S., Shenker, S., Joseph, B., Sanfilippo, P., Celniker, S.E., Graveley, B.R., and Lai, E.C. (2014). Genome-wide analysis of *Drosophila* circular RNAs reveals their structural and sequence properties and age-dependent neural accumulation. Cell Rep. *9*, 1966–1980.

Zhang, X.-O., Wang, H.-B., Zhang, Y., Lu, X., Chen, L.-L., and Yang, L. (2014). Complementary sequence-mediated exon circularization. Cell *159*, 134–147.